

Vibrational vs. electronic coherences in 2D spectrum of molecular systems

Vytautas Butkus^{1,2}, Donatas Zigmantas³, Leonas Valkunas^{1,2}, Darius Abramavicius^{1,4*}

¹Department of Theoretical Physics, Faculty of Physics,

Vilnius University, Sauletekio 9-III, LT-10222 Vilnius, Lithuania

²Center for Physical Sciences and Technology, Gostauto 9, LT-01108 Vilnius, Lithuania

³Department of Chemical Physics, Lund University, P.O. Box 124, 22100 Lund, Sweden and

⁴State Key Laboratory of Supramolecular Complexes,

Jilin University, 2699 Qianjin Street, Changchun 130012, PR China

The two-dimensional spectroscopy has recently revealed oscillatory behavior of excitation dynamics in molecular systems. However, in the majority of cases it is strongly debated if excitonic or vibrational wavepackets, or evidences of quantum transport have been observed. In this letter, the method for distinguishing between vibrational and excitonic wavepacket motion is presented, based on the phase and amplitude relationships of oscillations of distinct peaks, which has been revealed using fundamental analysis of two-dimensional spectrum of two representative systems.

Two-dimensional photon-echo (2DPE) spectroscopy is a powerful tool capable of resolving quantum correlations on the femtosecond timescale [1–3]. They appear as spectral beats in a number of molecular systems [3, 4], but the underlying processes are ambiguous. At first, the beats were attributed to the wave-like quantum transport with quantum coherences being responsible for an ultra-efficient excitation transfer [3–7]. Opposite phase beats in the spectral regions symmetric in respect of the diagonal line were indicated as an additional attribution of the observed spectral dynamics to the coherent energy transfer [8].

In general, molecular electronic transitions are coupled to various intra- and intermolecular vibrational modes. These vibrational energies are of the order of 100 - 3000 cm^{-1} , while the magnitude of resonant couplings J in the electronic aggregates (e.g. photosynthetic pigment-protein complexes or J-aggregates) are in the same range. Thus, vibronic and excitonic systems show considerable spectroscopic similarities, and electronic and/or vibrational beats should be anticipated in the 2DPE spectrum. Indeed, spectral beats originating entirely from a high-frequency vibrational wavepacket motion have been observed [9]. Turner et al [10] emphasized the difficulty of distinguishing electronic and vibrational coherences by comparing experimentally observed oscillatory evolution in the cross-peaks. Vibrations can also cause anticorrelation between amplitudes and the diagonal widths of isolated peaks [11]. Therefore, a highly-relevant question how vibrations interfere with electronic coherences is still open. Demonstration of the possibility to identify the origin of spectral beats from rephasing and non-rephasing components of the 2DPE spectrum of molecular aggregates is the issue of this letter.

We address this question by considering two generic model systems exhibiting distinct internal dynamics. A vibronic system is represented by two electronic states, $|g\rangle$ and $|e\rangle$ coupled to one-dimensional nuclear coordinate and denoted by a *displaced oscillator* (DO) model (Fig. 1a). The energy of the $|e\rangle$ state is shifted up by ex-

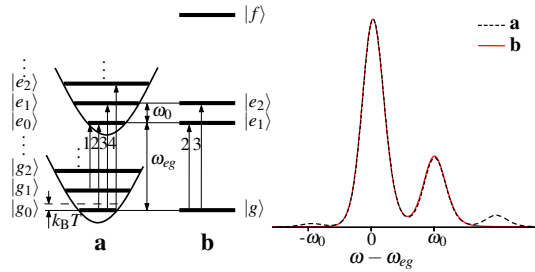


FIG. 1. Energy level structure of the displaced oscillator (a) and electronic dimer (b) and corresponding linear absorption spectra.

citation energy ω_{eg} and displaced by d with respect to the ground state $|g\rangle$ nuclear equilibrium. This setup results in two vibrational ladders of quantum sub-states $|g_m\rangle$ and $|e_m\rangle$, $m = 0 \dots \infty$, characterized by the Huang-Rhys (HR) factor $HR = d^2/2$ and vibrational frequency ω_0 . The simplest purely excitonic system, an *excitonic dimer* (ED), consists of two two-level chromophores (sites) with identical transition energies ϵ , coupled by the inter-site resonance coupling J . As a result, the ED has one ground state $|g\rangle$, two single-exciton states $|e_1\rangle$ and $|e_2\rangle$ with energies $\epsilon_{e_1, e_2} = \epsilon \pm J$, respectively, and a single double-exciton state $|f\rangle$ with energy $\epsilon_f = 2\epsilon - \Delta$, where Δ is the bi-exciton binding energy (Fig. 1b)[12].

The absorption spectrum of DO is determined by transitions from $|g_m\rangle$ vibrational ladder into $|e_m\rangle$ scaled by the Franck-Condon (FC) vibrational wavefunction overlaps [12]. Choosing $HR = 0.3$ and $k_B T \approx \frac{1}{3}\omega_0$ and assuming Lorentzian lineshapes with linewidth γ we get the vibrational progression in the absorption spectrum (dashed line in Fig. 1). The most intensive peaks at ω_{eg} and $\omega_{eg} + \omega_0$ correspond to 0-0 and 0-1 vibronic transitions. A similar peak structure is featured in the absorption of ED, where the spectrum shows two optical transitions $|g\rangle \rightarrow |e_1\rangle$ and $|g\rangle \rightarrow |e_2\rangle$, assuming both are allowed. Choosing $J = \omega_0/2$ and the angle φ between the chromophore transition dipoles $\pi/6$, and using the

adequate linewidth parameters, we get absorption lines (solid line in Fig. 1) that exactly match two strongest peaks of the DO. The absorption spectrum, as expected, cannot distinguish between these two internally different systems.

The 2DPE spectrum carries more information than the absorption. However, it entangles many contributions and characterization of ED and DO systems becomes troublesome. In order to unravel the 2DPE spectra we thus need to construct the entire 2D signal from scratch for both systems and recover the source of oscillations in the 2DPE spectrum for an arbitrary system. In the conventional scheme of the 2DPE signal generation, two primary excitation pulses with wavevectors \mathbf{k}_1 and \mathbf{k}_2 followed by pulse \mathbf{k}_3 are used. The signal is detected at the $\mathbf{k}_S = -\mathbf{k}_1 + \mathbf{k}_2 + \mathbf{k}_3$ direction. The order of \mathbf{k}_1 and \mathbf{k}_2 defines the rephasing configuration (\mathbf{k}_I) when \mathbf{k}_1 comes first and the non-rephasing configuration (\mathbf{k}_{II}) when \mathbf{k}_2 comes first.

Semiclassical perturbation theory reveals system-field interaction and evolution sequences encoding them through the Excited State Emission (ESE), Ground State Bleaching (GSB) and Excited State Absorption (ESA) contributions [13]. If we neglect the relaxation, the signals are given as a sum of resonant contributions of the type:

$$S(\omega_3, t_2, \omega_1) = \text{Re} \sum_n A_{(n)} \iint dt_1 dt_3 e^{+i\omega_3 t_3 + i\omega_1 t_1} \times [\pm G_3(t_3) G_2(t_2) G_1(t_1)]_{(n)}, \quad (1)$$

where the subscript n denotes different contributions. $A_{(n)}$ is the amplitude, given by the transition dipoles and excitation fields, the propagator of the density matrix for the j th ($j = 1, 2, 3$) time delay is of type $G_j(t_j) = \theta(t_j) \exp(-i\varepsilon_j t_j)$ ($\theta(t)$ is the Heaviside step-function), where ε_j is the system characteristic frequency equal to the energy gap ω_{ab} between the *left* and *right* states of the density matrix relevant to the interval t_j . ESE and GSB carry ‘+’ sign while ESA has ‘-’ overall sign. Fourier transforms in eq. 1 map the contributions to the frequency-frequency plot $(\omega_1, \omega_3) = (\mp|\varepsilon_1|, \varepsilon_3)$ (the upper sign is for \mathbf{k}_I , the lower – for \mathbf{k}_{II}). Diagonal peaks at $\omega_1 = \mp\omega_3$ are usually distinguished, while the anti-diagonal line is defined as $\mp\omega_1 + \omega_3 = \text{Const}$. The whole 2DPE signal becomes a function of t_2 : either oscillatory for coherences $|a\rangle\langle b|$ ($\varepsilon_2 = \omega_{ab} \neq 0$) in this time interval, or static for populations $|a\rangle\langle a|$ ($\varepsilon_2 = 0$).

To reveal oscillatory contributions in the DO and ED systems we have sorted out all contributions into either oscillatory or static as shown in Fig. 2a. If we consider only the two main vibrational levels in DO, the 2DPE spectrum will have only ESE and GSB contributions, while ED additionally has ESA. As a function of t_2 , the DO system has 8 oscillatory and 8 static contributions, which organize into six peaks, while the ED system has

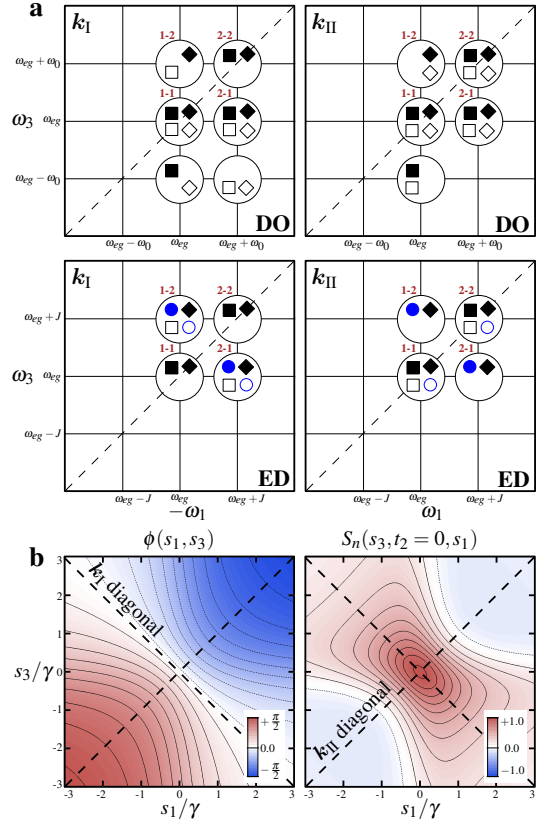


FIG. 2. (a) Scheme of contributions to 2DPE spectrum of the \mathbf{k}_I and \mathbf{k}_{II} signals for the reduced DO and ED ($\Delta = 0$) systems. The ESE contribution is indicated by squares, GSB – diamonds, ESA – circles. Solid symbols denote non-oscillatory contributions in t_2 , open – oscillatory in the form of $\pm \cos(\varepsilon_2 t_2)$, where $\varepsilon_2 = \omega_0$ for DO and $\varepsilon_2 = 2J$ for ED. (b) Phase ϕ of the contribution (Eq. 2) and peak lineshape S_n as a function of the shift from the peak center ($s_1 = s_3 = 0$) using relative coordinates. The diagonal lines of the \mathbf{k}_I and \mathbf{k}_{II} contributions to the 2D spectra are shown by dashed lines. Peaks are labelled in plots as “1-1”, “1-2”, etc.

only 4 oscillatory and 8 static contributions which give four peaks. Four additional oscillatory contributions in the DO system come from the coherence propagation in the ground state, while this part of system evolution is absent in the ED system. The net result is that the diagonal peaks in \mathbf{k}_I and cross-peaks in \mathbf{k}_{II} signals are non-oscillatory in the ED, while all peaks except the upper diagonal peak in \mathbf{k}_I are oscillatory in the DO. We thus find significant differences in oscillatory-peak positions between ED and DO systems.

An additional ingredient is a phase of oscillation. To reveal that, Eq. (1) can be analytically integrated for $G_j(t_j) \propto \exp(-i\varepsilon_j t_j - \gamma_j t_j)$. For a single contribution S_n giving rise to a peak at $(\omega_1, \omega_3) = (\mp|\varepsilon_1|, \varepsilon_3)$ we shift the frequency axes to the peak center ($\omega_1 \pm |\varepsilon_1| = s_1$, $\omega_3 - \varepsilon_3 = s_3$) and for $\gamma \approx \gamma_1 \approx \gamma_3$ we get the analytical

peak lineshape

$$S_n(s_3, t_2, s_1) = e^{-\gamma_2 t_2} \frac{A_n \chi(s_1, s_3) \cos(|\varepsilon_2| t_2 + \phi(s_1, s_3))}{(s_1^2 + \gamma^2)(s_3^2 + \gamma^2)}, \quad (2)$$

where

$$\chi(s_1, s_3)^2 = [\gamma^2 - s_1 s_3]^2 + \gamma^2 (s_3 + s_1)^2, \quad (3)$$

$$\phi(s_1, s_3) = \text{sgn}(\varepsilon_2) \arctan\left(\frac{\gamma(s_1 + s_3)}{(s_1 s_3 - \gamma^2)}\right). \quad (4)$$

The phase $\phi(s_1, s_3)$, and the lineshape for $A_n = 1$ and $t_2 = 0$ are shown in Fig. 2c. At the center of the peak ($s_1 = s_2 = 0$), we have $\chi = 1$ and $\phi = 0$, leading to $S_n \propto \cos(|\varepsilon_2| t_2)$. However, for ($s_1 \neq 0, s_2 \neq 0$) we find $S_n \propto \cos(|\varepsilon_2| t_2 + \phi(s_1, s_3))$ with $\phi(s_1, s_3) \neq 0$. Thus, *the displacement from the peak center determines the phase of the spectral oscillations*. Note that the sign of the phase ϕ is opposite for the peaks above ($\varepsilon_2 < 0$) and below ($\varepsilon_2 > 0$) the diagonal line, and *this applies for all contributions*.

However, the contributions blend into specific peaks, thus it is more important to characterize distinct peaks. Assuming that all dephasings are similar, different contributions to the same peak will have the same spectral shape and they can be added up. We can then simplify the 2DPE plot by writing the signal as a sum of peaks, which have static (from populations) and oscillatory (from coherences) parts:

$$S(\omega_3, t_2, \omega_1) = e^{-\gamma_2 t_2} \sum_{i,j} L_{ij}(\omega_1, \omega_3) \times [A_{ij}^P + A_{ij}^C \cdot \cos(|\omega_{ij}| t_2 + \phi_{ij}(\omega_1, \omega_3))]. \quad (5)$$

Here ω_{ij} is the characteristic oscillatory frequency of a peak (ij), $A_{ij}^P(t_2)$ and $A_{ij}^C(t_2)$ are orientationally-averaged slow-varying amplitudes (rise or decay) of population and coherence contributions, respectively. Note that the coherences can be electronic as in ED or vibrational as in DO model. The spectral lineshape is given by $L_{ij}(\omega_1, \omega_3)$. Here we now clearly identify the oscillatory amplitude and its phase for a specific peak.

To apply this expression for our system, we assume a typical situation where the laser pulses are tuned to the center of the absorption spectrum and the limited bandwidth selects the two strongest absorption peaks. In the 2DPE spectra two diagonal and two off-diagonal peaks for ED and DO are observed. Indices i and j in Eq. (5) run over the positions of the peaks and thus can be (1,1), (1,2), (2,1), and (2,2). For clarity we study the spectral dynamics with t_2 at the short delays, $t_2 \ll \gamma^{-1}$, and use notations A, L for the \mathbf{k}_I signal and \tilde{A}, \tilde{L} for the \mathbf{k}_{II} signal. The transition dipole properties of the ED results in the picture where all static amplitudes of the ED are positive and $A_{11}^P = \tilde{A}_{11}^P$, $A_{22}^P = \tilde{A}_{22}^P$, $A_{12}^P = A_{21}^P = \tilde{A}_{21}^P = \tilde{A}_{12}^P$. The oscillatory amplitudes are equal: $A_{12}^C = A_{21}^C = \tilde{A}_{11}^C = \tilde{A}_{22}^C$. The spectral beats

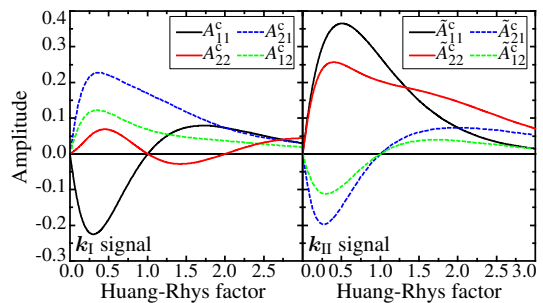


FIG. 3. Amplitudes of oscillating contributions of 2D spectra of monomer with vibrations for \mathbf{k}_I and \mathbf{k}_{II} signal.

with t_2 can thus have only the same phases in the rephasing or non-rephasing spectrum, when measured at peak centers. Additionally the oscillatory ESE and ESA parts in ED cancel each other if $\Delta = 0$ and their broadening is equal. As the amplitude relationships do not depend on coupling J and transition dipole orientations, all ED systems should behave similarly. By studying the whole parameter space, it can also be shown, that these amplitude-relationships will be of the same phase for a hetero-dimer since they do not depend on the coupling strength or orientations of transition dipoles.

The amplitude-relationships, however, are different for the DO system. The oscillatory amplitudes are plotted in Fig. 3 as a function of the HR factor, where now we include all vibrational levels in the $|g_m\rangle$ and $|e_m\rangle$ ladders. For \mathbf{k}_I , the amplitudes A_{11}^C and A_{22}^C maintain the opposite sign when $HR < 2$ and are both positive when $2 < HR < 3$ (note that $A_{22}^C = 0$ when only two vibrational levels are considered in Fig. 2b). The oscillation amplitudes A_{11}^C and A_{22}^C change sign at $HR = 1$. Amplitudes A_{12}^C and A_{21}^C are always positive. Spectrum oscillations with t_2 for both diagonal peaks in the \mathbf{k}_{II} signal will be in-phase for the whole range of the HR factor. The same pattern holds for the 1-2 and 2-1 cross-peaks, which will oscillate in-phase, but will be of opposite phase compared to the diagonal peaks in the region of $HR < 1$. Note that the sign of amplitudes changes with the HR factor, since the overlap integral between vibrational wavefunctions can be both positive and negative. The amplitudes of static contributions are positive in the whole range of parameters and are identical for both \mathbf{k}_I and \mathbf{k}_{II} signals.

We thus find very different behaviour of oscillatory peaks of DO and ED systems. The above analysis applies for the central positions of the peaks, which may be difficult to determine if the broadening is large. Note that the phase ϕ varies from $-\pi/2$ to $+\pi/2$ (Eq. (2) and Fig. 2c) when probing in the vicinity of the peak. However, $\phi = 0$ along the diagonal line for \mathbf{k}_I and along the anti-diagonal line for \mathbf{k}_{II} . These lines can thus be used as guidelines for reading phase relations of distinct peaks in the 2DPE spectrum. For instance, the two diagonal

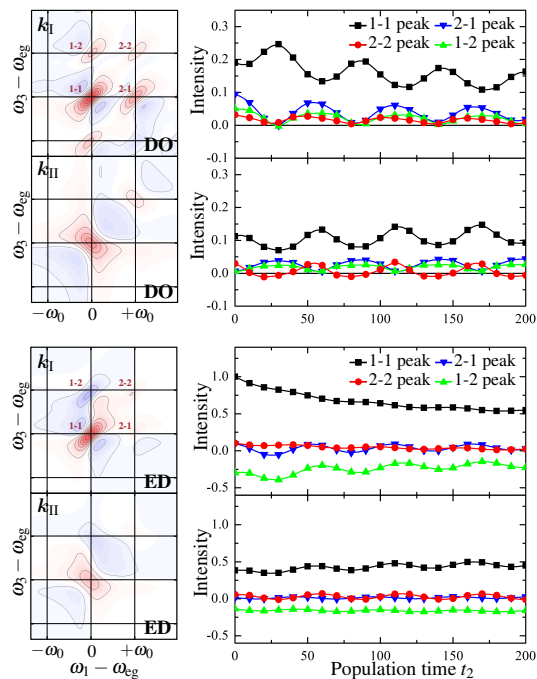


FIG. 4. 2DPE spectra and peak intensities of the DO and ED as the function of population time t_2 , of the k_{I} and k_{II} signals. Spectra are normalized to the maxima of the total spectra of the DO and ED, independently.

peaks can be calibrated by reading their amplitudes at the diagonal line, or the two opposite cross-peaks can be compared by drawing anti-diagonal lines.

The 2DPE spectra for both DO and ED systems calculated by including phenomenological relaxation and Gaussian laser pulse shapes [13, 14] are plotted in Fig. 4. The structure and t_2 evolution of the spectra illustrates the dynamics discussed above and clearly shows distinctive spectral properties of the vibronic vs. electronic system: (i) diagonal peaks in the k_{I} signal are oscillating in DO, but only exponentially decaying in ED (the oscillatory traces come from the overlapping tails of off-diagonal peaks), (ii) the relative amplitude of oscillations is much stronger in DO as compared to ED, where the ESA and ESE cancellation suppresses the oscillations and static contributions, (iii) opposite oscillation phases are observed in DO, while all peaks in ED oscillate in-phase.

The up-to-date experiments are capable of creating pulse spectral bandwidth of 1500 cm^{-1} and more [11]. Thus, the overtones in DO can be excited and beats of $n\omega_0$ frequencies (n is integer) observed. These may become important in the case of large HR factors. Such frequencies are absent in the ED system, since only one oscillatory frequency, equal to $2J$ is available.

The analysis presented in this letter provides a clear physical picture of electronic and vibronic coherence beatings in 2DPE spectra. We are able to discriminate weakly damped electronic and vibronic coherent

wavepackets in molecular systems based on fundamental theoretical considerations. Oscillatory dynamics may also be observed due to quantum transport in electronic aggregates caused by a strong system coupling with an overdamped bath, which leads to oscillations of diagonal peaks, *phase-shifted by $\frac{\pi}{2}$* with respect to the cross-peaks [7]. Dynamics of diagonal peaks and cross-peaks as well as relative phase between them can now be classified for vibrational and excitonic systems as follows. (i) Static diagonal peaks and oscillatory off-diagonal peaks signify pure electronic coherences, not involved in energy transport. (ii) Oscillatory diagonal peaks in accord with off-diagonal peaks (0 or π phase relationships) signify vibronic origins. (iii) The $\pi/2$ phase relation between diagonal and off-diagonal peaks could be a signature of quantum transport. This classification will help to clarify possible misinterpretations of experimentally observed beatings in molecular systems and identify spectral beats in photosynthetic aggregates and to finally answer the question of importance of electronic coherences in excitonic energy transfer, its efficiency and robustness.

This research was funded by the European Social Fund under the Global Grant measure.

* darius.abramavicius@ff.vu.lt

- [1] P. F. Tian, D. Keusters, Y. Suzuki, and W. S. Warren, *Science* **300**, 1553 (2003).
- [2] X. Li, T. Zhang, C. N. Borca, and S. T. Cundiff, *Phys. Rev. Lett.* **96**, 057406 (2006).
- [3] G. S. Engel, T. R. Calhoun, E. L. Read, T. K. Ahn, T. Mančal, Y. C. Cheng, R. E. Blankenship, and G. R. Fleming, *Nature* **446**, 782 (2007).
- [4] E. Collini and G. D. Scholes, *Science* **323**, 369 (2009).
- [5] F. Caruso, A. W. Chin, A. Datta, S. F. Huelga, and M. Plenio, *J. Chem. Phys.* **131**, 105106 (2009).
- [6] P. Rebertrost, M. Mohseni, and A. A. Guzik, *J. Phys. Chem. B* **113**, 9942 (2009).
- [7] G. Panitchayangkoon, D. V. Voronine, D. Abramavicius, J. R. Caram, N. Lewis, S. Mukamel, and G. S. Engel, *Proc. Nat. Acad. Sci. USA* p. (in press) (2011).
- [8] E. Collini, C. Y. Wong, K. E. Wilk, P. M. G. Curmi, P. Brumer, and G. D. Scholes, *Nature* **463**, 644 (2010).
- [9] A. Nemeth, F. Milota, T. Mančal, V. Lukeš, J. Hauer, H. F. Kauffmann, and J. Sperling, *J. Chem. Phys.* **132**, 184514 (2010).
- [10] D. B. Turner, K. E. Wilk, P. M. G. Curmi, and G. D. Scholes, *J. Phys. Chem. Lett.* **2**, 1904 (2011).
- [11] N. Christensson, F. Milota, J. Hauer, J. Sperling, O. Bixner, A. Nemeth, and H. F. Kauffmann, *J. Phys. Chem. B* **115**, 5383 (2011).
- [12] H. van Amerongen, L. Valkunas, and R. van Grondelle, *Photosynthetic Excitons* (World Scientific, Singapore, 2000).
- [13] D. Abramavicius, L. Valkunas, and S. Mukamel, *Europhys. Lett.* **80**, 17005 (2007).
- [14] D. Abramavicius, V. Butkus, J. Bujokas, and L. Valkunas, *Chem. Phys.* **372**, 22 (2010).